antibonding with regard to the metal d_{z^2} orbitals while the bottom corresponds to an essentially nonbonding interaction of the d_{z^2} metal orbital. The z^2 exchange pathway that occurs in the compounds investigated in this paper as well as in other compounds where octahedral chromophores share either opposite corners or opposite trigonal faces[30,33] appears to be one of the most efficient for Ni(II) coupled systems. In particular, it leads to stronger antiferromagnetic interactions than the $x^2 - y^2$ exchange pathway, which predominates when octahedral chromophores share opposite edges.[21,28] In contrast, it is now well established that the x^2–y^2 exchange pathway is particularly efficient in Cu(II) coupled systems.[2-4,35,40]

Acknowledgment. This work was technically and financially supported by the CNRS, the DGRST, and the DESR.

Registry No. $Ni(N_2C_2H_8)_2(NO_2)(PF_6)$, 80642-84-8; $Ni(N_2C_2H_8)_2(NO_2)(ClO_4)$, 30496-54-9; $Ni(N_2C_2H_8)_2(NO_2)(I_3)$, 80642-85-9.

Supplementary Material Available: Listings of structure factor amplitudes (5 pages). Ordering information is given on any current masthead page.

(40) J. J. Girerd, O. Kahn, and M. Verdaguer, *Inorg. Chem.*, **19**, 274 (1980).

Contribution from the Department of Chemistry,
University of Notre Dame, Notre Dame, Indiana 46556

Triborane. A Transition-Metal Ligand or Heterocluster Fragment?

CATHERINE E. HOUSECROFT and THOMAS P. FEHLNER*

Received October 5, 1981

The nature of the metal–boron bonding in three metallaboranes containing triborane fragments possessing significantly different geometrical structures is explored by means of the extended Hückel technique. It is demonstrated that important aspects of the nature of the structures of these three metallaboranes can be understood on the basis of the frontier orbital behavior of the triborane fragments as a function of triborane geometry. This work confirms the relationship of one metallaborane to organometallic allyl complexes and explores the ligand behavior of the $B_3H_8^-$ ion toward metals. In addition a trend in ligand vs. cluster behavior for the three triborane fragments is established.

Introduction

It is well established that boranes can serve as ligands to metals in low-valence states in a manner parallelling organic fragments.[1] Moreover, metallaboranes have been classified according to the ligand behavior of the borane fragment with respect to the metal.[2] On the other hand, metallaboranes can be usefully considered as clusters, a description also encompassing organometallic compounds.[3] The difference between the two views is partly semantic, but it is of interest to explore the implied real differences in terms of metallaboranes containing the same size borane fragment in dissimilar bonding arrangements.

The triborane fragment is the simplest polyborane in which three distinct bonding modes toward metal are exhibited. These are distinguished by significant changes in the geometry of the borane fragment as established crystallographically. In the first mode, of which $(Me_2PPh)_2PtB_3H_7$ is the exemplar,[4] the triborane, B_3H_7, binds to the metal in a structural form analogous to the allyl cation ($C_3H_5^+$), hence the term "borallyl" (Figure 1). Further evidence for this bonding mode comes from NMR studies of $Ir(B_3H_7)(CO)H(PPh_3)_2$.[5] The bonding of larger borane fragments to transition metals via three borons has also been described as allyl-like.[6] The second known form of triborane bonding to transition metals is found in compounds containing $B_3H_8^-$, a species that can be isolated as uncomplexed ligand as well.[7] Structurally characterized examples include $(Ph_3P)_2CuB_3H_8$,[8] $[(CO)_4CrB_3H_8]^-$,[9] $(CO)_4MnB_3H_7Br$,[10] and $Be(B_3H_8)_2$.[11,12] The bonding in the first three has been likened to that of the *nido*-borane, B_4H_{10}, in which the metal fragment replaces a "wing-tip" BH_2^+ in the borane "butterfly" (Figure 2).[1] Note that $B_3H_8^-$ can be formally generated from B_3H_7 by the addition of H^- to the central boron. The third established bonding mode for triboranes is found in the ferraborane, $(CO)_6Fe_2B_3H_7$, a formal dimetallapentaborane[13] (Figure 3). The triborane ligand is positioned such that all three boron atoms are associated with the apical iron atom, while two basal borons are associated with the remaining iron via two bridging hydrogens. The binding of this triborane to a diiron fragment has been examined earlier,[13,14] and it is clear that the most useful description of the structure of this compound is as a formal derivative of B_5H_9; i.e., neither the borallyl nor the $B_3H_8^-$ descriptions serve as good models. This is most dramatically evidenced by the BBB angle of the triborane being 113° in the borallyl compound, 60° in the $B_3H_8^-$, derivatives and 94° in this ferraborane.

In this work we explore these three distinct binding modes exhibited by triboranes using qualitative molecular orbital methods in the manner of Hoffmann.[15] By considering the compounds containing triborane as being formed from appropriate metal and borane fragments, it is possible to examine

(1) Dunks, G. B.; Hawthorne, M. F. In "Boron Hydride Chemistry"; Muetterties, E. L., Ed.; Academic Press: New York, 1975; p 383. Wegner, P. A. *Ibid.*, p 431.
(2) Greenwood, N. N. *Pure Appl. Chem.* **1977**, *49*, 791.
(3) Wade, K. *J. Chem. Soc., Chem. Commun.* **1971**, 792. Mingos, D. M. P. *Nature (London), Phys. Sci.* **1972**, *236*, 99. Rudolph, R. W. *Acc. Chem. Res.* **1976**, *9*, 446. Grimes, R. N. *Ibid.* **1978**, *11*, 420.
(4) Guggenberger, L. J.; Kane, A. R.; Muetterties, E. L. *J. Am. Chem. Soc.* **1972**, *94*, 5665.
(5) Greenwood, N. N.; Kennedy, J. D.; Reed, D. *J. Chem. Soc., Dalton Trans.* **1980**, 196.
(6) Hilty, T. K.; Thompson, D. A.; Butler, W. M.; Rudolph, R. W. *Inorg. Chem.* **1979**, *18*, 2642.
(7) Peters, C. R.; Nordman, C. E. *J. Am. Chem. Soc.* **1960**, 82, 5738.
(8) Lippard, S. J.; Melmed, K. M. *Inorg. Chem.* **1969**, *8*, 2755.
(9) Guggenberger, L. J. *Inorg. Chem.* **1970**, *9*, 367.
(10) Chen, M. W.; Calabrese, J. C.; Gaines, D. R.; Hillenbrand, D. F. *J. Am. Chem. Soc.* **1980**, *102*, 4928.
(11) Calabrese, J. C.; Gaines, D. F.; Hildebrandt, S. J.; Morris, J. H. *J. Am. Chem. Soc.* **1976**, *98*, 5489.
(12) Other modes of bonding of the $B_3H_8^-$ species such as tridentate (Hildebrandt, S. J.; Gaines, D. F.; Calabrese, J. C. *Inorg. Chem.* **1978**, *17*, 790) or as a dimetal bridge (Chen, M. W.; Gaines, D. F.; Hoard, L. G. *Ibid.* **1980**, *19*, 2989) have been observed.
(13) Haller, K. J.; Andersen, E. L.; Fehlner, T. P. *Inorg. Chem.* **1981**, *20*, 309.
(14) Andersen, E. L.; DeKock, R. L.; Fehlner, T. P. *Inorg. Chem.* **1981**, *20*, 3291.
(15) Hoffman, R. *Science (Washington, D.C.)* **1981**, *211*, 995 and references therein.

0020-1669/82/1321-1739$01.25/0

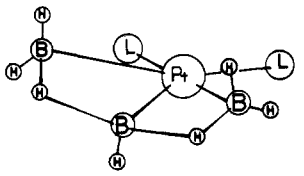

Figure 1. Schematic drawing of the skeletal structure of $(Me_2PPh)_2PtB_3H_7$.[4] The positions of the hydrogen atoms were not located in the crystal structure determination.

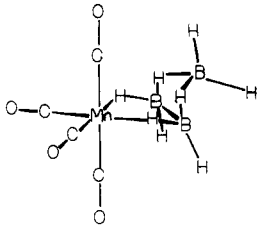

Figure 2. The molecular structure of $(CO)_4MnB_3H_8$, based on the structure of $(CO)_4MnB_3H_7Br$.[10]

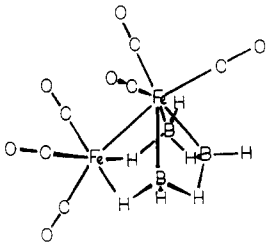

Figure 3. The molecular structure of $(CO)_6Fe_2B_3H_7$.[13]

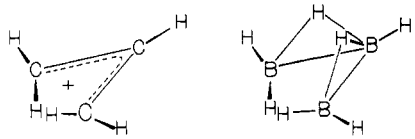

Figure 4. Comparison of the structures of $C_3H_5^+$ and the "borallyl" form of B_3H_7.

the bonding tendencies of the three known structural forms of the triborane fragment and the manner in which they combine with transition metals. Besides allowing us to analyze the ability of this borane to adapt itself to the requirements of the transition metal, it allows us to comment effectively on the true distinction between metallaboranes as metal complexes vs. clusters.

Borallyl: B_3H_7 (115°). The frontier orbitals of the allyl cation (Figure 4)[16] consist of a bonding, out-of-plane, π-type HOMO and a nonbonding, out-of-plane LUMO (Figure 5). The interaction of these orbitals with those of a metal fragment to form an allyl complex has been presented previously[17] where it has been noted that it is the nonbonding orbital of the allyl fragment that is important in controlling the allyl orientation with respect to metal fragment. Borallyl, B_3H_7 (115°) (Figure 4), is structurally similar to allyl cation except in two respects. There are two out-of-plane bridging hydrogens, and the BB distances are significantly longer than the CC distances (1.39 vs. 1.89 Å). In addition, the presence of bridging hydrogens in the borallyl ligand reduces the symmetry from C_{2v} to C_s, leaving only a plane of symmetry common to both.

The results of extended Hückel calculations on borallyl are schematically presented in Figure 5, where they are compared

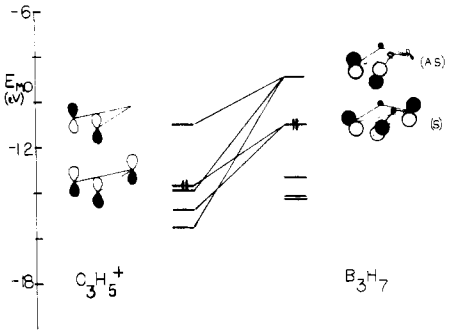

Figure 5. Comparison of the frontier orbital structures of $C_3H_5^+$ and B_3H_7 (120°), "borallyl". The lines show the orbitals of $C_3H_5^+$ with which the HOMO and LUMO of a B_3H_7 correlate. Only the 2p contributions of C and B are indicated.

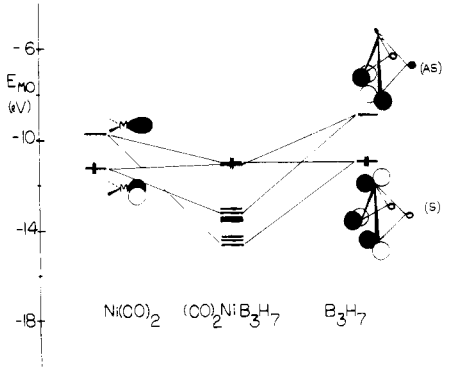

Figure 6. Orbital interaction diagram for $(CO)_2NiB_3H_7$ (120°).

to a similar calculation for the allyl cation.[18] The HOMO and LUMO of the former are quite noticeably higher in energy; however, they retain roughly the same energy splitting. The HOMO of each ligand is symmetric with respect to the common plane of symmetry while the LUMO in both cases is antisymmetric with respect to this plane. Thus, in terms of potential interaction with a metal fragment, both species have similar requirements. A closer look at the borallyl frontier orbitals reveals some significant perturbations vis-à-vis the allyl cation. The bridging hydrogen character is spread over several MO's, and the net effect on any one orbital is relatively small. On the other hand, the reduction in symmetry resulting from the introduction of the hydrogen bridges allows out-of-plane and in-plane B_{2p} mixing. Because of this, there is a large tilting of the 2p contributions in the HOMO and a smaller, but significant, tilting in the LUMO such that these two MO's point toward a potential metal atom on the side of the plane of the boron atoms opposite the bridging hydrogens (Figure 5). In terms of metal bonding, this effect should compensate for the larger BB distance relative to the CC distance in $C_3H_5^+$.

So that the interaction with a metal fragment could be explored, extended Hückel calculations were performed on $(CO)_2NiB_3H_7$, $(CO)_2NiC_3H_5^+$, and the $Ni(CO)_2$ fragment.[19] So that this could be done, the geometry of the complex was idealized with the metal atom equidistant from each boron atom such that the metal atom is placed in an approximate square-planar environment. These restrictions cause the plane of the B_3 unit to be at 130° to the plane containing the Ni-$(CO)_2$ fragment with the central boron shifted away from the carbonyl groups, thereby approximating the observed structure.[9] Note that the bridge hydrogens project out of the BBB plane away from the metal atom. The results on the allyl

(16) It is convenient to consider the allyl ligand as a cation. At the extended Hückel level there are no essential differences between the comparison $B_3H_7/C_3H_5^+$ and $B_3H_7^{2-}/C_3H_5^-$.
(17) Schilling, B. E. R.; Hoffmann, R.; Faller, J. W. *J. Am. Chem. Soc.* **1979**, *101*, 592.
(18) Some calculations on the preferred structure of free B_3H_7 have appeared: Brown, L. D.; Lipscomb, W. N. *Inorg. Chem.* **1977**, *16*, 1. Dewar, M. J. S.; McKee, M. L. *Ibid.* **1978**, *17*, 1569.
(19) Elian, M.; Hoffmann, R. *Inorg. Chem.* **1975**, *14*, 1058.

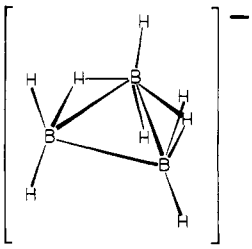

Figure 7. C_{2v} structure of $B_3H_8^-$ that serves as the "idealized" structure of the B_3H_8 fragment in $(CO)_4MnB_3H_8$.

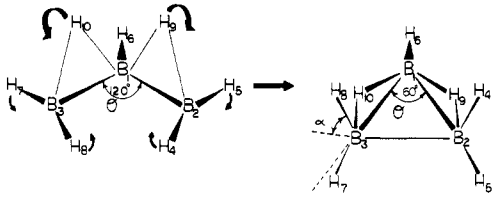

Figure 8. Generation of B_3H_7 (60°) from B_3H_7 (120°). The angle θ is in the BBB plane and the angle α measures the dihedral angle of the plane containing a BH_2 group with the plane containing the three borons.

complex are consistent with those published earlier, and those on the borallyl complex (schematically shown in Figure 6) are consistent with the expectations noted above. In particular, the major interactions in forming $(CO)_2NiB_3H_7$ are with the HOMO and LUMO of the metal and ligand fragments; however, there does seem to be more extensive scrambling of orbital character than is the case with the allyl complex. Finally, as is the case with organic ligands,[15] it is the interaction of the antisymmetric LUMO of borallyl with the HOMO of the $Ni(CO)_2$ fragment that has a large role in determining the orientation of the B_3 framework with respect to the $Ni(CO)_2$ plane.

Octahydrotriborate(1−): B_3H_7 (60°) + H^-. The $B_3H_8^-$ species (Figure 7) can be generated from borallyl in the following manner beginning with an idealized B_3H_7 (120°) (see Calculations). By decreasing the BBB bond angle (θ) from 120 to 60°, while twisting the BH_2 groups and the bridging hydrogens through an angle α equal to 90° such that the terminal hydrogens take up out-of-plane positions and the bridging hydrogens in-plane positions (Figure 8), one generates the hypothetical B_3H_7 (60°) shown. Pertinent orbital energies from extended Hückel calculations on this system are shown in Figure 9, where they are compared to those for B_3H_7 (120°). In agreement with a more extensive study of B_3H_7 (60°),[18,20] the LUMO consists of an orbital that is mainly out-of-plane 2p on the boron with a single terminal hydrogen (B_1 in Figure 8). Adding the base H^- to B_3H_7 (60°) to form $B_3H_8^-$ (Figure 7) creates another filled MO which is derived from the LUMO of B_3H_7 (60°) thereby effectively stabilizing it. As the next lowest lying empty orbital of B_3H_7 (120°) has been greatly destabilized by the change in geometry required to generate B_3H_7 (60°), $B_3H_8^-$ is found to have a very large HOMO–LUMO gap (Figure 9). The size of this gap is consistent with the fact that $B_3H_8^-$ is found as a free ligand.[7] It also suggests that $B_3H_8^-$ should not be a very good π acceptor, a fact that is of significance with regard to potential interactions with metals.[21]

The HOMO of $B_3H_8^-$ (and B_3H_7 (60°)) is B_2–B_3 (Figure 8) bonding, symmetric with respect to the molecule's plane

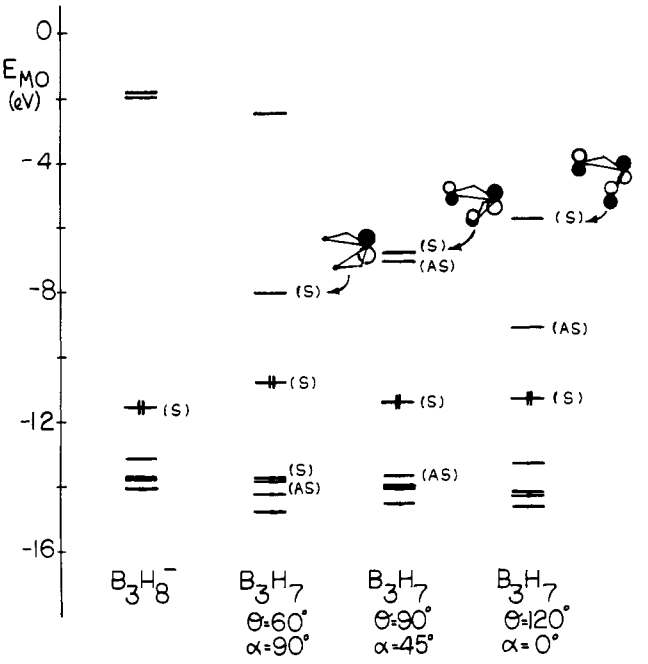

Figure 9. Comparison of the frontier orbital structures of B_3H_7 (120°), B_3H_7 (90°), B_3H_7 (60°), and $B_3H_8^-$. Sketches for other orbitals will be found in Figures 5 and 11.

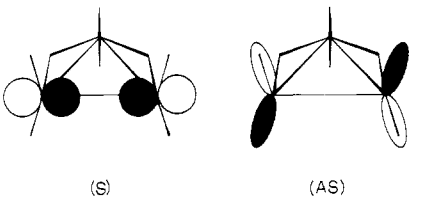

Figure 10. Pictorial representation of the HOMO and the highest lying antisymmetrical filled orbital of $B_3H_8^-$.

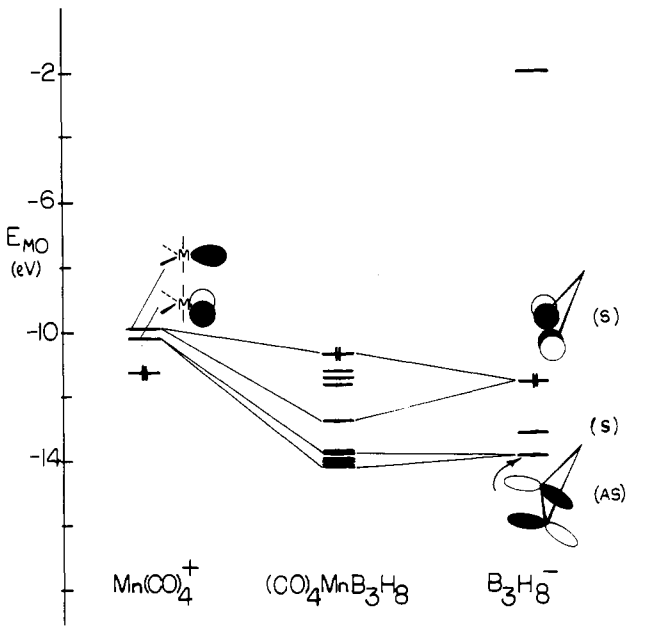

Figure 11. Orbital interaction diagram for $(CO)_4MnB_3H_8$.

of symmetry, and in the BBB plane (Figure 10). The next highest filled orbital is B_1–B_2 and B_1–B_3 bonding, symmetric, and in the BBB plane. These two orbitals correlate with the highest lying, degenerate, Walsh orbitals of the isoelectronic cyclopropane molecule, the two bridging hydrogens in $B_3H_8^-$ serving to remove the degeneracy. In contrast to borallyl vs. $C_3H_5^+$, the in-plane bridging hydrogens do not cause in-plane

(20) Pepperberg, I. M.; Halgren, T. A.; Lipscomb, W. N. *Inorg. Chem.* **1977**, *16*, 363. See also: Pepperberg, I. M.; Dixon, D. A.; Lipscomb, W. N.; Halgren, T. A. *Ibid* **1978**, *17*, 586.

(21) Information on the electronic structure of $B_3H_8^-$ has already appeared: Lipscomb, W. N. In "Boron Hydride Chemistry"; Muetterties, E. L., Ed.; Academic Press: New York, 1975; p 39. References 18 and 20.

and out-of-plane mixing and the orbital structure of $B_3H_8^-$ remains reminiscent of that of cyclopropane. Consideration of the triborane fragment alone does not permit the determination of the orbital or orbitals important in regard to the orientation of the $B_3H_8^-$ fragment with respect to the metal fragment (Figure 2). When bound to a metal, the symmetry of the $B_3H_8^-$ fragment is reduced from C_{2v} to C_s. Therefore we have carried out calculations on $B_3H_8^-$ in the C_s geometry exhibited by this fragment in B_4H_{10} (Figure 2) and have demonstrated that the idealized (C_{2v}) geometry serves to represent well the qualitative properties of the $B_3H_8^-$ fragment.

Using the idealized geometry for $B_3H_8^-$, we have carried out an extended Hückel calculation on $(CO)_4MnB_3H_8$. The results (Figure 11) demonstrate that the HOMO of the triborane interacts with the symmetric empty orbital of $Mn(CO)_4^+$ as expected. In addition, it is found that the empty, low-lying, antisymmetric metal orbital interacts significantly with the third highest filled MO of $B_3H_8^-$ (Figure 10), which is an out-of-plane orbital and the highest lying antisymmetric filled orbital. The participation of the metal and ligand antisymmetrical orbitals in the formation of the complex allows the orientation of the triborane with respect to the metal fragment to be understood. For effective orbital overlap, the plane of the triborane unit must be tilted acutely with respect to the $Mn(CO)^+_4$ vertical axis and the B_2–B_3 bond must lie parallel with a line drawn between the two equatorial carbonyl carbon atoms (Figure 2). In addition, as the antisymmetric triborane orbital has significant contributions from the 1s functions of the terminal hydrogens attached to B_2 and B_3, the participation of hydrogens in the borane metal interaction via Mn–H–B bridges becomes natural. Finally, when $B_3H_8^-$ is distorted to the C_s structure as it is found in B_4H_{10} (see above), this antisymmetric orbital is polarized toward the terminal hydrogens on the same side of the BBB plane as the bridging hydrogens, thus rationalizing the orientation in $(CO)_4MnB_3H_8$ (Figure 2).

B_3H_7 (90°). The geometry of the B_3H_7 fragment as found in $(CO)_6Fe_2B_3H_7$, B_3H_7 (90°), can be generated by the same process used to form B_3H_7 (60°) from borallyl (Figure 8). However, the opening and twisting process is terminated at a BBB angle of 90° and a twist angle α of 45°. This positions each plane containing a BH_2 group at 45° to the plane of the B_3 fragment and each plane containing two borons and the hydrogen bridging them also at 45° to the B_3 plane.

An extended Hückel calculation on this system (viz., B_3H_7 (90°)) demonstrates similarities and differences between the orbital properties of both B_3H_7 (120°) and B_3H_7 (60°). The energies of the frontier orbitals of all three species are compared in Figure 9 (see earlier figures for orbital drawings). The HOMO in all three cases is symmetric with respect to the plane of symmetry and is B_2–B_3 bonding (or would be for B_3H_7 (90°) and B_3H_7 (120°) if the borons were within bonding distance). However, the HOMO of B_3H_7 (90°) is tilted similarly to that of B_3H_7 (120°) (see above) rather than being in-plane as is the situation with B_3H_7 (60°). B_3H_7 (90°) has a filled, antisymmetric orbital similar to that in B_3H_7 (60°), i.e., $B_3H_8^-$, at about the same energy. This orbital is oriented for interacting with a metal on the side of the BBB plane opposite to that of the bridging hydrogens. The differences are more evident in the nature of the unfilled orbitals. B_3H_7 (90°) has two low-lying empty orbitals of nearly equal energy. One is antisymmetric and similar to the LUMO in B_3H_7 (120°); however, the tilting with respect to a line perpendicular to the BBB plane has substantially increased. The other is symmetric and related to the LUMO for B_3H_7 (60°) and the second lowest unfilled orbital of B_3H_7 (120°). The main difference lies in the relative contributions of B 2p on B_1 vs. B_2 and B_3. Thus, in terms of bonding with metal fragments, B_3H_7 (90°) possesses requirements that are a hybrid of those of B_3H_7 (120°) and B_3H_7 (60°). That is, the metal fragment must have at least one symmetric low-lying empty orbital (with respect to the symmetry plane of the triborane). In addition, an antisymmetric empty low-lying orbital would facilitate bonding with B_2 and B_3 via M–H–B bridges. At least one symmetric and one antisymmetric high-lying filled orbitals are required as well. To go beyond these elementary predictions is difficult but it does seem reasonable that the complex demands of B_3H_7 (90°) could most easily be met with a multinuclear metal fragment.

Table I. Triborane Fragment Charges on Metalloboranes

compd	Mulliken charge on B_3H_x	compd	Mulliken charge on B_3H_x
$(CO)_4MnB_3H_8$	0.80–	$(CO)_6Fe_2B_3H_7$[a]	0.15–
$(CO)_4NiB_3H_7$	0.36–		

[a] Reference 14.

Extended Hückel calculations carried out previously on $(CO)_6Fe_2B_3H_7$[14] exhibit three high-lying filled metal–boron interaction orbitals that clearly correlate with the two lowest lying empty orbitals and the HOMO of B_3H_7 (90°). In addition, one can identify filled orbitals in $(CO)_6Fe_2B_3H_7$ containing Fe–H–B character which are analogous to those found in $(CO)_4MnB_3H_8$. Despite these observations there is no clean cut way in which the frontier orbitals of B_3H_7 (90°) can be correlated with the orbital properties of the $Fe_2(CO)_6$ fragment.[22-24] Thus, in our judgment, it is not too useful to consider $(CO)_6Fe_2B_3H_7$ as a metal–ligand complex.

Ligand vs. Cluster Behavior. The hallmark of a ligand is the ability to preserve, to a large extent, its identity while bound in a metal complex. On the other hand, the hallmark of a cluster fragment is the merging of its identity with those of the other fragments which make up the cluster. A "perfect" ligand only contributes to the electric field at the metal atom, and the qualitative orbital description of the ligand remains unchanged. Good approximations of such ligands will be found only in ionic compounds. A cluster fragment can only behave in a "perfect" manner in a homoatomic system where the cluster fragment orbitals will be identical in energy and properties. These qualitative observations provide two guides with which to judge cluster vs. ligand behavior in general and may be used to evaluate the metallaboranes discussed above.

There is no definitive measure of the mixing between ligand and metal fragment orbitals, and such mixing depends on the calculational technique used. However, in a relative sense and within the context of a single type of calculation, the present results suggest that scrambling of metal and ligand components increases in the order $(CO)_2NiC_3H_5^+ < (CO)_2NiB_3H_7 \approx (CO)_4MnB_3H_8 < (CO)_6Fe_2B_3H_7$, suggesting that the cluster bonding description becomes increasingly more realistic in that order. As a "perfect" ligand will have no low-lying empty orbitals, the density of empty, low-lying orbitals also provides a guide to the clustering tendency of a given fragment. Figures 5 and 9 suggest that with respect to a given metal, the tendency toward cluster bonding increases in the order $B_3H_8^- < B_3H_7$ (120°) $\approx C_3H_5^+ < B_3H_7$ (90°).

A less subjective measure of cluster vs. ligand behavior is found in the charge distributions of the metallaboranes. The extent that the electronic charge of the metallaborane is polarized between the metal and borane fragments serves to define how closely the compound mimics the "perfect" homoatomic cluster.[25] The metal and triborane fragment

(22) Anderson, A. B. *Inorg. Chem.* **1976**, *15*, 2598.
(23) Thorn, D. L.; Hoffmann, R. *Inorg. Chem.* **1978**, *17*, 126.
(24) Andersen, E. L.; Fehlner, T. P.; Foti, A. E.; Salahub, D. R. *J. Am. Chem. Soc.* **1980**, *102*, 7422.

Table II. Molecular Parameters for Idealized Geometries

parameter (X = C or B)	$C_3H_5^+$ [a]	B_3H_7 (borallyl)	B_3H_7 (Figure 9)	$B_3H_8^-$	$(CO)_4MnB_3H_8$ [b]	$(CO)_2NiB_3H_7$ [c]
X_1-X_2 or X_1-X_3, [d] Å	1.39	1.89	1.80	1.80	1.80	1.89
X-H_{term}, Å	1.09	1.19	1.19	1.19	1.19	1.19
X-$H_{bridge-X}$, Å		1.32	1.32	1.32	1.32	1.32
M-X_2 or M-X_3, Å					2.36	2.23
M-X_1, Å					3.36	2.23
M-$H_{bridge-X}$, Å					1.84	
M-CO, Å					1.83	1.84
MC-O, Å					1.13	1.15
X_2-X_1-X_3, deg	115	115	60, 90, 120	60	60	120
H_{term}-X-H_{term}, deg	120	120	120	120	120	120
X_1-H_{bridge}-X_2, deg		91.4	86	86	86	91.4
X_1-H_{bridge}-X_3, deg						
M-H_{bridge}-X, deg					99.8	

[a] Reference 8. [b] Reference 10. [c] Reference 9. [d] Notation as in Figure 8.

Table III. Extended Hückel Exponents

atom	orbital	Slater exponent	H_{ii}, eV
H[a]	1s	1.3	−13.60
B[b]	2s	1.3	−14.01
	2p	1.3	−8.28
C[a]	2s	1.625	−21.40
	2p	1.625	−11.40
O[a]	2s	2.275	−32.30
	2p	2.275	−14.80
Mn[c]	3d	2.60	−10.67
	4s	0.97	−9.38
	4p	0.97	−5.72
Ni[c]	3d	2.60	−13.50
	4s	0.97	−10.43
	4p	0.97	−6.09

[a] Reference 28. [b] Reference 29. [c] Reference 30.

Mulliken charges from the calculations on the metallaboranes are given in Table I where it may be seen that, in terms of polarity, cluster behavior increases in the order $(CO)_4MnB_3H_8 < (CO)_2NiB_3H_7 < (CO)_6Fe_2B_3H_7$. Thus all three views are consistent in suggesting $(CO)_6Fe_2B_3H_7$ as the compound exhibiting the highest degree of cluster behavior.

In the simple triborane fragment dicussed here one finds unprecedented versatility[26] in accomodating transition-metal fragments by relatively simple changes in the skeletal geometry. These changes alter the frontier MO's, significantly allowing interaction with three (at least) types of metal fragments. On the one hand the borane fragment can be usefully termed a "η^3-borallyl ligand", B_3H_7 (120°), and on the other, a "bidentate ligand", $B_3H_8^-$. In the middle lies a fragment whose bonding is not realistically ligand-like at all, but is, instead, decidedly "cluster-like".

Calculations. Structures of fragments and complexes are idealized and, where possible, were based on experimentally determined parameters. The basic bond distances used are given in Table II. The extended Hückel calculations[27] employed Slater functions, and the orbital exponents and diagonal matrix elements used are given in Table III. The arithmetic mean Wolfsberg–Hemholz approximation with $K = 1.75$ was used.

Acknowledgment. The support of the National Science Foundation under Grant CHE 78-11600 and discussions with Professor R. L. DeKock are gratefully acknowledged. We thank the University of Notre Dame Computer Center for providing computing time.

Registry No. $(CO)_2NiB_3H_7$, 80662-69-7; $(CO)_4MnB_3H_8$, 53801-97-1; $(CO)_6Fe_2B_3H_7$, 71271-99-3.

(25) This does not imply a uniform charge distribution in homonuclear clusters but only that for a given borane fragment interacting with transition metals the net electronic charge relative to the metal will decrease with an increase in cluster behavior.
(26) The formal similarity to σ- and π-allyl must be noted, however.

(27) Hoffmann, R. *J. Chem. Phys.* **1963**, *39*, 1397; Hoffmann, R.; Lipscomb, W. N. *Ibid.* **1962**, *36*, 3489; **1962**, *37*, 2872.
(28) Burdett, J. K. *J. Chem. Soc., Dalton Trans.* **1977**, 424.
(29) Basch, H.; Viste, A.; Gray, H. B. *Theor. Chim. Acta* **1964**, *3*, 458.
(30) The diagonal matrix elements of iron[28] were changed in proportion to the orbital ionization energies of manganese and nickel. See: Ballhausen, C. J.; Gray, H. B. "Molecular Orbital Theory"; W. A. Benjamin: New York, 1964; p 122.